Supporting Information

High photoactive heterojunction based on g-C_3N_4 nanosheets decorated with dendritic zinc (II) phthalocyanine through axial coordination and its ultrasensitive enzyme-free sensing for choline

Hong Dai [a*], Shupei Zhang [a], Guifang Xu [a], Yiru Peng [a], Lingshan Gong[a], Xiuhua Li[a], Yilin Li [a], Yanyu Lin [a,b], Guonan Chen [b*]

a College of Chemistry and Chemical Engineering, Fujian Normal University, Fuzhou

350108, P. R. China

b Ministry of Education Key Laboratory of Analysis and Detection for Food Safety,

and Department of Chemistry, Fuzhou University, Fuzhou 350002, P. R. China

EXPERIMENTAL SECTION

Materials and Reagents. Choline and melamine were obtained from Sigma-Aldrich (USA) and were used without further purification. N-Pentanol and 1,8-diazabicyclo-(5,4,0)-undec-7-ene (DBU) were purchased from Aldrich. Phosphate buffer solution (PBS) was prepared by mixing stock solution of 0.1 M NaH_2PO_4 and 0.1 M Na_2HPO_4 and adjusting the pH. Other reagents were of analytical regent grade. The water used for the preparation of the solution was purified using a Water purifier (China) purification system.

Apparatus. Amperometric i-t Curve and electrochemical impedance spectroscopy (EIS) were performed with a CHI 760 electrochemical analyzer (Shanghai Chenghua Instrument Co., China). Amperometric i-t Curves were carried out with a three-electrode system comprising a platinum wire auxiliary electrode, Ag/AgCl reference electrode (sat. KCl) and a glassy carbon electrode (GCE, φ3mm) which served as the working electrode. The pH measurements were carried out on PHS-3C exact digital pH metre (Shanghai Leici Co. Ltd., China), which was calibrated with standard pH buffer solutions. Photoelectrochemical measurements were performed with a homemade photoelectrochemical system.

Synthesis of Dendritic Zinc (II) Phthalocyanine. 1-generations cyano-terminated dendritic ether (0.4 g, 0.8 mmol) mixed with $Zn(OAc)\cdot 2H_2O$ (0.04 g, 0.20 mmol) in n-pentanol (20 mL) and they were heated at 404 K, then some drops of DBU were added. The mixture was stirred at 423K overnight. Then remove volatiles under reduced pressure to obtain a greenish blue solid, which was chromatographed twice with ethyl acetate/hexanes (9:1(v/v)) as eluent. The obtained product dissolved in a minimum amount of tetrahydrofuran，then adding MeOH (60 mL) and H_2O (140 mL) to induce precipitation. The greenish blue solid of ZnPc(CN)8 was obtained after filtration and drying in vacuo. A mixture of compound ZnPc(CN)8 (800 mg) in 2 M NaOH (60 mL) was heated at 398 K with stirring for 7 h, and the precipitation formed in 1 M HCl (200 mL) and was filtered off. The resulting blue solid containing with NaOH dissolved in water (60 mL), and several drops of 1 M HCl were added until the pH reached 7. Ethanol (200 mL) was then added to precipitate the salt, and the mixture stood overnight. The corresponding product DZP was collected by filtration and dried in vacuo. The scheme for synthesis of dendritic zinc (II) phthalocyanine was showed in the Fig.s-1. In addition, both the FTIR spectra and 1H NMR spectra of dendritic zinc (II) phthalocyine was also displayed in the Fig. S2, indicating that the dendritic zinc (II) phthalocyine was successfully synthesized.

Synthesis of g-C_3N_4 Nanosheets. g-C_3N_4 nanosheets was prepared as previous works.[4a] In short, 10.0g of white melamine powder was placed into a porcelain boat and heated at 823K for 4 h in a tube furnace under open air condition. Then the production was cooled to room temperature to obtain the primrose yellow g-C_3N_4 product. At last, it was prepared for the further use.

Preparation of Modified Glassy Carbon Electrode. Before modification, the bare glassy carbon electrode (GCE, 3 mm in diameter) was polished with 0.3 ,0.05μm alumina particles on chamois leather in sequence, then washed sequentially with doubly distilled water in an ultrasonic bath and dried in air before use. For preparation the modified electrode, the 2 mg/mL g-C_3N_4 solution was mixed with 2 μM DZP (1:2(v/v)) under stirring for 24 h at room temperature and the resulting solution was centrifuged at 15000 rpm for 10 min. Then the precipitate was dispersed in water after it dried at room temperature. Afterward, with a microinjector, 4 μL of the solution was deposited on the fresh prepared GCE surface, and kept in an over at 60℃ for 25min.

Sample Preparation. Solution containing honey sample was prepared as followed. Firstly, 0.2661 g (200μL) honey was dissolved in 1 mL methanol with vigorous sonication. Then the resulting suspension was centrifuged at 15000 rpm for 30 min. Then the liquid phase was collected for subsequent application. Before experiment, 1 mL resultant solution was mixed with 199 mL 0.1 M PBS (pH 7.0).

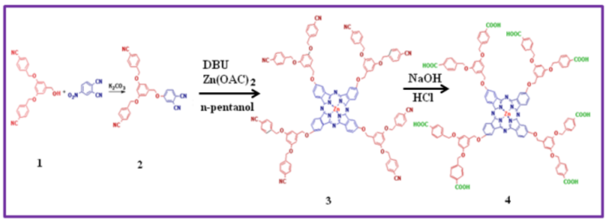

Fig. S1 The scheme for synthesis of dendritic zinc (II) phthalocyanine

Characterization of dendritic zinc (II) phthalocyanine

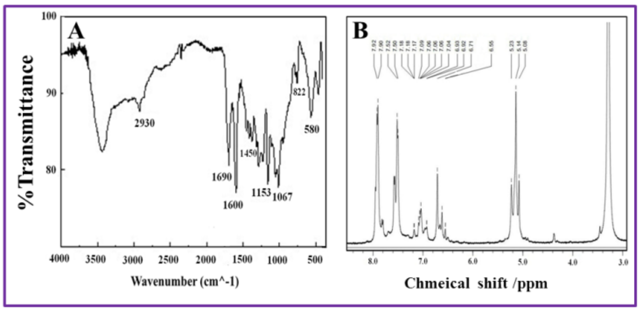

Fig. S2 (A)FTIR spectra of dendritic zinc(II) phthalocyine (B) 1H NMR spectra of dendritic zinc(II) phthalocyine.

Fig. S2A displayed the FTIR spectra of DZP, which showed that the characteristic of the phthalocyanine ring structure at 1600 cm-1, 1450 cm-1 and1500 cm-1. Additionally, the peaks at 1067 cm^{-1} and 1153 cm^{-1} corresponded the vibration absorption peaks of the C-O-C of aryl ether and the characteristic absorption peaks of C=O of carboxy appeared at 1690 cm^{-1} which can be attributed to the cyano group was completely hydrolyzed to carboxyal groups were observed. Furthermore, 1H NMR spectroscopy was shown in the Fig. S2B, which can be used to monitored DZP. It could be seen that the signal for all of the prepared phthlocyanine, which were classified six groups in aromatic. The proton singals for phthalocyanine ring H4, H5, H6 were at δ6.92 ~ 6.93 ppm (d, J = 4Hz, 4H), 7.04 ~ 7.06 ppm (d, J = 8Hz, 4H) and 7.18 ppm (s, 4H), respectively. And the singals atδ7.90 ~ 7.92 ppm (d, J = 8Hz, 16H) and 7.50 ~ 7.52 ppm (d, J = 8Hz, 16H) came from the H7 and H8 of external branches proton. The substituents of H3 and H2 proton on aryl ether produced the singals for protons at δ 6.71 ppm (s，8H) and 6.55 ppm (s, 4H). In the hydrocarbon, there were three kinds of proton signals: δ = 5.23, 5.14 and 5.08 ppm, which ascribed to the three aryl ether chain methylene. The integral calculus ratio of the proton signals in aromatic hydrocarbon and hydrocarbon was 2.5 to 1.1, consistenting with the theoretical value.

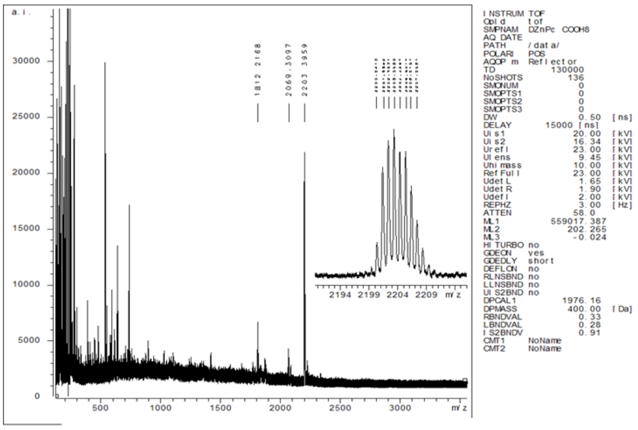

Fig. S3 MALDI-TOF spectrum of dendritic zinc(II) phthalocyine

Moreover, the MALDI-TOF was used to prove the purity of dendritic zinc(II) phthalocyine. As shown in Fig. S3, MS (MALDI-TOF) (m /z), 2201. Found: 2203 $[M+2]^+$. Accordingly, the characterized results indicated that dendritic zinc (II) phthalocyanine was successfully prepared.

Fig. S4 IPCE spectra of g-C_3N_4 and g-$C_3N_{4/}$DZP and the inset is the IPCE comparing

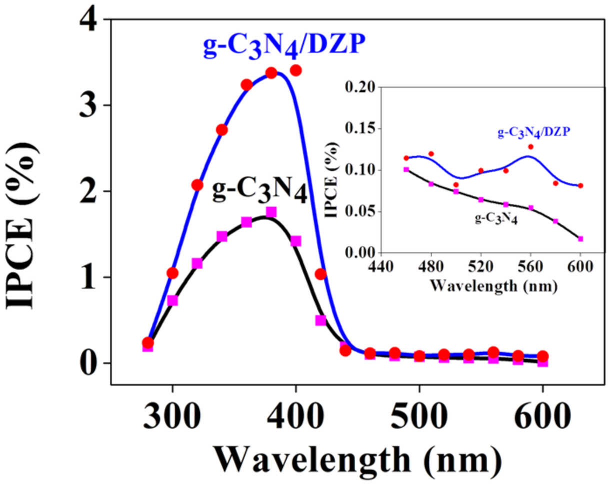

in visible light region.

To evaluate the photoelectrochemical performance of g-C_3N_4 and g-C_3N_4/DZP, the incident photon-to-current conversion efficiency (IPCE) were exhibited in Fig. S4. The IPCE is defined as following:

$$IPCE(\%) = \frac{1240 \times j}{P \times \lambda} \times 100$$

where j is the photocurrent density (mA cm^{-2}), P is the power of monochromatic light irradiated on the electrode (mW cm^{-2}) and λ is the incident photon wavelength (nm). The measurement was performed under 0 V bias vs. Ag/AgCl. As demonstrated in Fig. S4, the IPCE of g-C_3N_4 increased from 0.19% to 1.76% at 380 nm and in the visible light region g-C_3N_4 possessed good light harvesting. Therefore, in this manuscript, we used the visible light as the irradiated light source. Besides, the g-C_3N_4/DZP had the highest absorbance in 400 nm, and the IPCE had an obviously increasing in the near infrared especially in 560 nm. The result demonstrated DZP successfully coupled with g-C_3N_4 through axial coordination and the forming of p-n junction resulted in the improved photocatalytic performance.

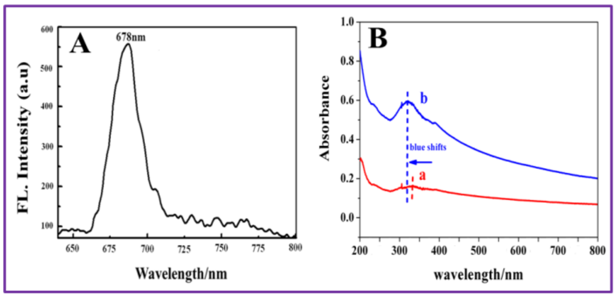

Fig. S5 (A)The fluorescence spectra of DZP excitation at 290 nm, and (B) UV/Vis spectra of (a) g-C_3N_4, (b) g-C_3N_4/DZP solution.

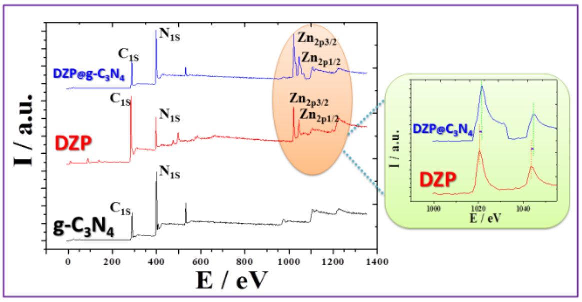

Fig. S6 Survey XPS spectra of g-C_3N_4, dendritic zinc (II) phthalocyanine and they formed composite.

As shown in Fig. S6, g-C_3N_4 were composed of C and N elements. From the high resolution XPS spectra of Zn 2p, the signals of DZP can be observed, attributing to the Zn 2p3/2 and 2p1/2 core-level energies, which are typical positions for zinc compounds. While, for the DZP and g-C_3N_4 formed composite, the binding energies of Zn 2p3/2 and 2p1/2 both increased around 0.75 eV when compared with that case of DZP. This could be attributed to the change of the electron density around the nucleus. Thus, it was a valid evidence of the strong interaction between zinc and g-C_3N_4. Moreover, the N 1s binding energy of this composite increased 1eV when compared with that of DZP and g-C_3N_4, which provided further evidence for axial coordination between the DZP and carbon nitride nanosheets. All in all, the XPS findings were in accord with the UV/Vis observations, indicating the existence of axial coordination between the DZP and g-C_3N_4 nanosheets.

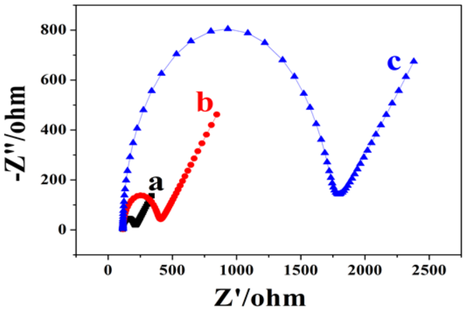

Fig. S7 Nyquist diagrams of electrochemical impedance spectra of various electrodes. Electrolyte：5×10^{-3} mol L^{-1} $[Fe(CN)_6]^{3-/4-}$ and 0.1 mol L^{-1} KCl. GCE (a), g-C3N4/GCE (b) and g-C3N4/ZnPc$(COOH)_8$/GCE (c).

The EIS measurement not only acted as an effective tool for characterizing the interface properties of electrodes but also was used to investigate the fabrication process. As the Fig. S7 shown, the impedance spectrum of the g-C_3N_4 modified electrode in 5×10^{-3} mol L^{-1} $[Fe(CN)_6]^{3-/4-}$ containing 0.1 mol L^{-1} KCl displayed a relatively larger semicircle (curve b) than the case of GCE. Comparing curve b, after the ZnPc$(COOH)_8$ dropped on the electrode surface the resistance Ret increased dramatically. It was attributed to the poor conductive properties of the ZnPc$(COOH)_8$, which can be explained that the electronegative ZnPc$(COOH)_8$ progressively obstruct the mass transport and electro transfer of the electrochemical probe $[Fe(CN)_6]^{3-/4-}$ to the electrode surface by elevating the hindrance effect.

Table S1 Comparable figures of determining choline

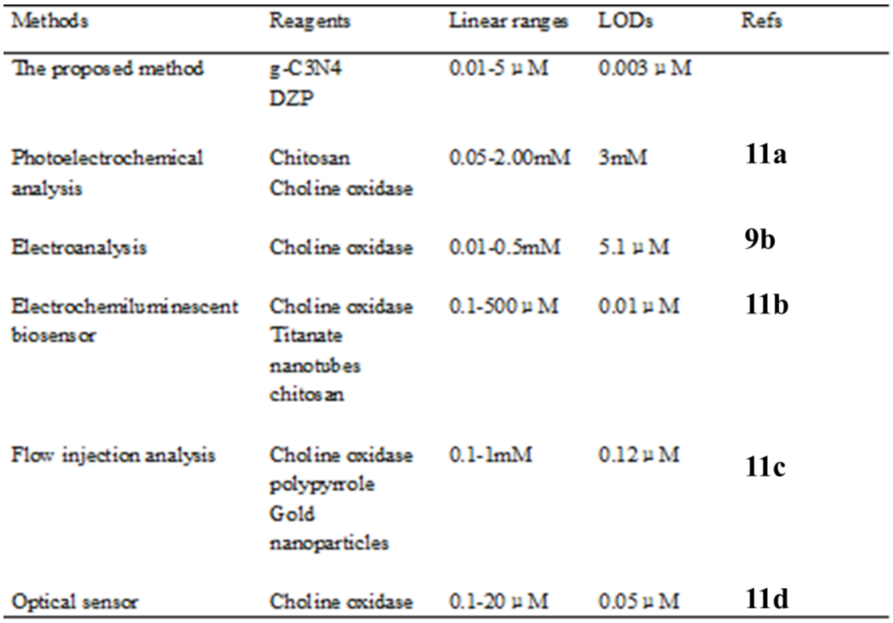

Methods	Reagents	Linear ranges	LODs	Refs
The proposed method	g-C3N4 DZP	0.01-5 μM	0.003 μM	
Photoelectrochemical analysis	Chitosan Choline oxidase	0.05-2.00mM	3mM	**11a**
Electroanalysis	Choline oxidase	0.01-0.5mM	5.1 μM	**9b**
Electrochemiluminescent biosensor	Choline oxidase Titanate nanotubes chitosan	0.1-500 μM	0.01 μM	**11b**
Flow injection analysis	Choline oxidase polypyrrole Gold nanoparticles	0.1-1mM	0.12 μM	**11c**
Optical sensor	Choline oxidase	0.1-20 μM	0.05 μM	**11d**

Table S2 Determination results of choline in honey

Sample	Found (mg/g)	Added (mg /g)	Total found (mg /g)	Recovery (%)
Honey1	0.0133	0.0545	0.0673	99.1
Honey2	0.0133	0.109	0.123	100.6